Novel factors modulating AGC kinase signaling-controlled polar auxin transport

Xiao, Y.

Chapter 3

PDK1 is part of an auxin-sensing rheostat controlling vascular differentiation

Yao Xiao[1], Remko Offringa[1*]

[1]Plant Developmental Genetics, Institute of Biology Leiden, Leiden University, Sylviusweg 72, 2333 BE, Leiden, The Netherlands.

[*]Author for correspondence: r.offringa@biology.leidenuniv.nl

Abstract

BREVIS RADIX (BRX) and PROTEIN KINASE ASSOCIATED WITH BRX (PAX) operate as a molecular rheostat in regulating PIN-FORMED (PIN) auxin efflux carrier activity during root protophloem differentiation. Elevated auxin levels decrease the plasma membrane abundance of BRX, thereby releasing PAX and allowing its activation leading to PIN phosphorylation and enhanced auxin efflux. However, how PAX itself is activated by phosphorylation is still unknown. Here we identified the 3'-*PHOSPHOINOSITIDE-DEPENDENT PROTEIN KINASE 1* genes *PDK1* and *PDK2* as novel protophloem regulatory genes. The *pdk1 pdk2* double loss-of-function mutant shows severe protophloem differentiation defects in the root and fragmented vein patterning in the cotyledons. By complementation analysis we prove that PDK1 is responsible for PAX activation by phosphorylation at Serine596 during vascular development, and that it does not require its phospholipid binding Pleckstrin Homology (PH) domain for this process. Our data indicates an important role for PDK1 in auxin-directed feedback signaling during vascular differentiation.

Introduction

Vascular tissues in land plants consist of phloem and xylem, two functionally distinct domains that provide highways interconnecting highly differentiated plant organs and tissues, allowing them to benefit from each other so that plants can efficiently grow and survive on land. Xylem is composed of dead cells at maturity and transports water and minerals taken up from the soil from the root to stems and leaves. In contrast, phloem consists of living cells that transport sap containing sugars, amino acids, hormones and other messenger molecules from source to sink organs (De Rybel et al., 2016).

During the past decades, numerous genes have been identified that regulate phloem differentiation and development (summarized in Anne and Hardtke, 2018). Apart from several downstream nuclear-localized transcriptional regulators, such as ALTERED PHLOEM DEVELOPMENT (APL) (Durner et al., 2003), AUXIN RESPONSE FACTORs (ARFs) (Marhava et al., 2018), SMAX1-LIKEs (SMXLs) (Wallner et al., 2017), NAC45/86 (Furuta et al., 2014) and PHLOEM EARLY DOFs (PEARs) (Miyashima et al., 2019), the upstream signaling pathways can be classified into five different groups: 1) the brassinosteroid (BR) signaling pathway involving the BRASSINOSTEROID INSENSITIVE 1/ -LIKE1/ -LIKE3 (BRI1/BRL1/BRL3) receptor kinases and the downstream BRASSINOSTEROID-INSENSITIVE 2 (BIN2) kinase (Anne et al., 2015; Kang et al., 2017); 2) the OCTOPUS *(OPS)* and OPS-LIKE2 pathway that promotes BR signaling by inhibiting BIN2 (Truernit et al., 2012; Anne et al., 2015; Ruiz Sola et al., 2017); 3) a signaling cascade involving CLAVATA3/ENDOSPERM SURROUNDING REGION 45 (CLE45), the receptor-like kinase BARELY ANY MERISTEM 3 (BAM3) and the MEMBRANE-ASSOCIATED KINASE REGULATOR 5 (MAKR5) (Kang and Hardtke, 2016; Hazak et al., 2017); 4) the auxin-dependent pathway involving BREVIS RADIX (BRX), PROTEIN KINASE ASSOCIATED WITH BRX (PAX) and the PIN FORMED (PIN) auxin efflux carriers (Scacchi et al., 2010; Marhava et al., 2018); 5) enzymes involved in phosphoinositide homeostasis, including the PHOSPHATIDYLINOSITOL-4-PHOSPHATE 5-KINASEs (PIP5Ks) and the inositol polyphosphate 5'-phosphatases COTYLEDON VASCULAR PATTERN 2 and CVP2-LIKE1 (CVP2/CVL1) (Mouchel et al., 2004; Carland and Nelson, 2009; Rodriguez-Villalon et al., 2015). These pathways play parallel roles in controlling vascular differentiation, but there is clear cross-talk between them and most mutants in the corresponding genes display defects in root protophloem development.

The Arabidopsis primary root has been widely used as a model for studying phloem function and development at the molecular level, because of its easy experimental accessibility (Anne and Hardtke, 2018). In the root meristem zone, the stem-cell niche is maintained by high auxin levels, whereas relatively lower auxin levels keep the stem cell daughter cells in the dividing state before cell specification. The subsequent differentiation of the specified cells is accompanied by a gradual increase in auxin concentration. Expression of a constitutively active version of the ARF5/MONOPTEROS (MP) in protophloem sieve elements (PPSEs) using the CVP2 promoter results in accelerated PPSE differentiation, emphasizing that accurate modulation of the auxin response is a critical step in the protophloem differentiation process (Bauby et al., 2007; Marhava et al., 2018). This modulation of the auxin response is mainly achieved through the activity of the PIN auxin efflux carriers PIN1, PIN3, and PIN7, which are predominantly located at the rootward (basal) side of root stele cells, and control the

auxin concentration in the individual cell types by directing the auxin flux toward the root tip (Feraru and Friml, 2008; Marhava et al., 2018).
The auxin transport activity and polarity of these PIN1-type carriers are controlled by AGC kinase family members through direct phosphorylation of specific serine residues in their large central hydrophilic loop (PIN-HL). Phosphorylation by the AGC kinases PINOID (PID), WAG1 or WAG2 regulates PIN polarity (Friml et al., 2004; Dhonukshe et al., 2010; Huang et al., 2010), whereas phosphorylation by the PID, D6PK or D6PK-LIKE (D6PKL) AGC kinases has been reported to enhance PIN-mediated auxin efflux capacity (Barbosa et al., 2014; Zourelidou et al., 2014). Recently, the D6PK/D6PKL-related kinase PAX was identified from a screen for BRX interactors by co-immunoprecipitation mass spectrometry (Marhava et al., 2018). PAX is specifically expressed in the developing protophloem and xylem axis of the root, where it co-localizes with PIN1 and BRX at the basal side of cells. At lower auxin levels, BRX interacts with PAX at the plasma membrane and inhibits its activation, resulting in reduced PIN-mediated auxin efflux and leading to an increase in the cellular auxin concentration. These higher auxin levels induce movement of BRX from the PM to the nucleus, thereby releasing PAX and allowing it to be activated by phosphorylation at Serine596 (S^{596}). Activated PAX subsequently enhances auxin efflux by phosphorylating PIN proteins, again leading to reduced cellular auxin levels. Loss-of-function mutants in the *PAX* gene have a shorter primary root. The root phenotype is much weaker compared to that of *brx* and *ops* mutants, but *pax* roots have similar gaps in the PPSE differentiation zone, which is caused by the failure of cell differentiation and characteristic cell-wall thickening (Marhava et al., 2018).
In Chapter 2 we reported on the strong developmental defects of the Arabidopsis double loss-of-function mutant in the 3-PHOSPHOINOSITIDE-DEPENDENT KINASE-1 (PDK1) encoding genes *PDK1* and *PDK2*. Interestingly, the root defects of this mutant strongly resemble those observed for the *pax*, *brx*, and *ops* loss-of-function mutants. Moreover, PAX has previously been shown to be activated by PDK1 by phosphorylation at serine^{596} (S^{596}) (Zegzouti et al., 2006; Gray et al., 2013). Here we show that PDK1 functions directly upstream of PAX as an activator in the auxin-sensing rheostat during root protophloem differentiation. Unexpectedly, PDK1 does not require its phospholipid binding PH domain for this activator function.

Results

Vascular defects underly the short root phenotype of the *pdk1 pdk2* mutant

Seedlings of the *pdk1 pdk2* loss-of-function mutant develop fused or aberrantly positioned cotyledons and a significantly shorter primary root that starts to show agravitropic growth around 7 days after germination (Figure 1A, B) (Chapter 2). The specific expression pattern of *PDK1* and *PDK2* in (pro)vascular tissues from early embryo development suggested a role for these genes in vascular development (Figure 1C, D) (Chapter 2). PDK1 has previously been shown to be an activator of the AGC kinase PAX *in vitro* (Zegzouti et al., 2006; Gray et al., 2013). Since *pax* mutants also have a short root because of defects in protophloem differentiation (Marhava et al., 2018), we investigated *pdk1 pdk2* roots for vascular defects. Protophloem differentiation in *pdk1 pdk2* roots was indeed disturbed, leading to a high frequency of gaps in PPSEs (Figure 1E, F, G). These gaps were absent and root growth was restored to wild-type levels in *pPDK1::YFP:PDK1* (*PDK1*) complemented double mutant lines

(Figure 2A, B), indicating that defects in protophloem differentiation are caused by *pdk1 pdk2* loss-of-function and that they underlie the short root phenotype of mutant seedlings.

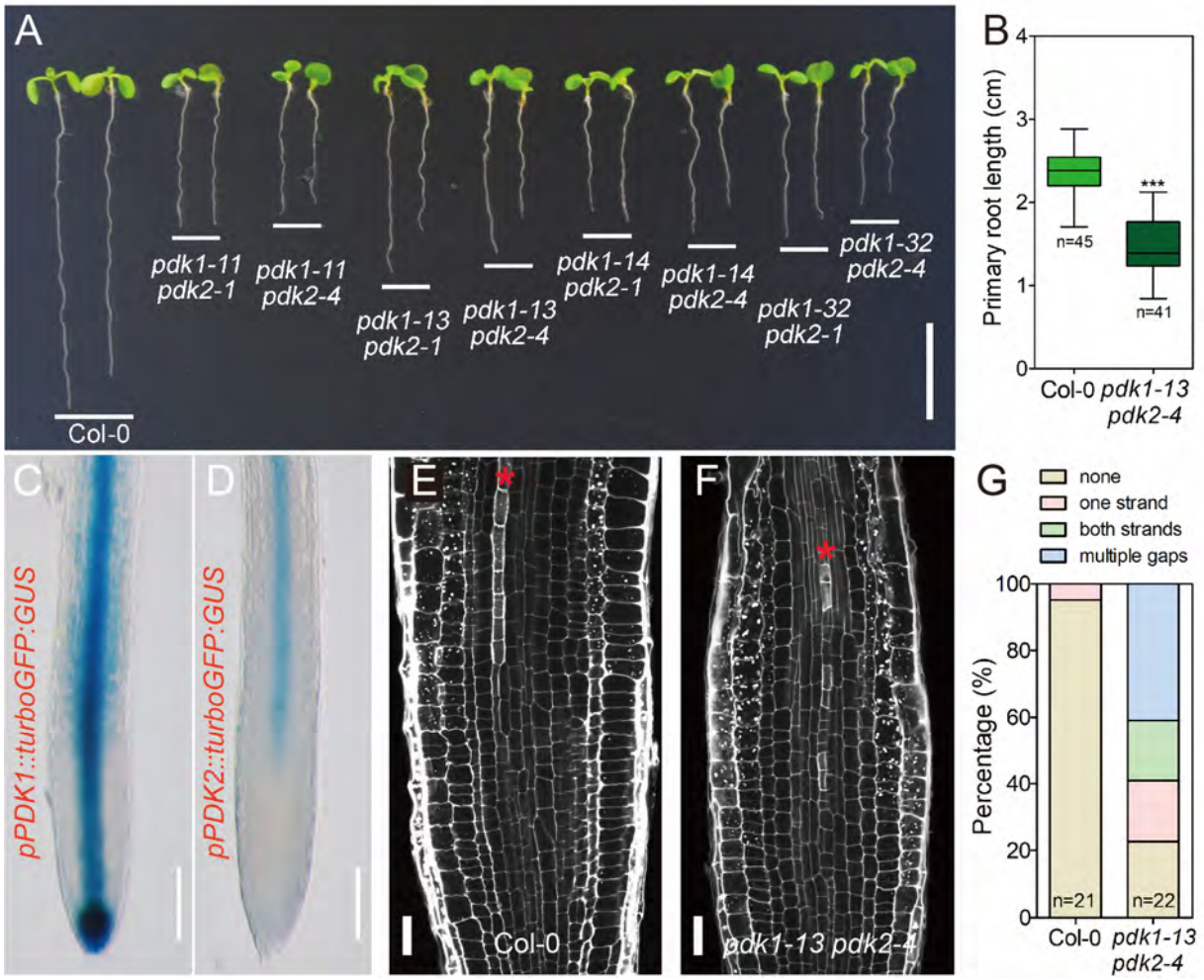

Figure 1. *PDK1* and *PDK2* are expressed in primary root vascular tissue to control phloem development-dependent root elongation. A, 7-day-old seedling phenotype of wild type (Col-0) and different *pdk1 pdk2* mutant combinations. Bar = 1 cm. B, primary root length of 7-day-old wild type (Col-0) and *pdk1-13 pkd2-4* (*t*-test, ***p<0.001), whiskers: Min to Max. C and D, DIC microscopy images of roots of 5-day-old *PDK1* (C) and *PDK2* (D) *promoter::turboGFP-GUS* seedlings stained for GUS activity. Bar = 0.1 mm. E and F, Confocal sections of mPS-PI stained wild-type (Col-0, E) and *pdk1-13 pdk2-4* (F) roots. The protophloem cell layer is indicated with a red asterisk. Bar =10 µm. G, Quantification of gaps in PPSEs in wild-type and *pdk1-13 pdk2-4* roots. The number of observed roots is indicated in each bar.

PDK1 is the PAX activator in the auxin-sensing rheostat regulating PPSE differentiation

Phosphorylation of PAX at S^{596}, which is a PDK1 *in vitro* target (Zegzouti et al., 2006; Gray et al., 2013), has been reported to be induced by auxin to fine tune auxin concentrations during PPSE differentiation (Zegzouti et al., 2006; Gray et al., 2013; Marhava et al., 2018). Introduction of a construct containing a *PDK1* promoter driven *YFP:PAX(S596D)* fusion gene (*PAX(SD)*) in the *pdk1 pdk2* mutant background completely restored protophloem differentiation and primary root growth (Figure 2A, B, C). Root gravitropic growth was also partially restored in *PAX(SD) pdk1 pdk2* seedlings (Figure S1M-O). *PDK1* promoter-driven expression of a *YFP*- wild-type *PAX* fusion (*PAX*) only rescued primary root growth when *PAX* was expressed at a very high level (Figure 2A, D). In comparison, the *PAX(SD)* construct only

required low expression for complementation. These results indicate that PDK1 is an activating kinase in the rheostat and also suggest that either PAX, like PID, is able to sufficiently auto-activate when expressed at high levels, or that another less efficient kinase can activate PAX when it is abundantly expressed. *PAX(SD) pdk1 pdk2* or *PAX pdk1 pdk2* seedlings still exhibited a strongly decreased lateral root development, similar to the *pdk1 pdk2* mutant, either with a shorter (#9-7 and #13-3) or comparable (#4-7) primary root (Figure S1J-L). The reduced lateral root initiation is likely to be caused by a lack of activation of other PDK1 substrates, most likely the D6PK/D6PKLs, and indicates that PAX has a specific role in vascular development, but cannot completely take over the role of these other AGC kinases.

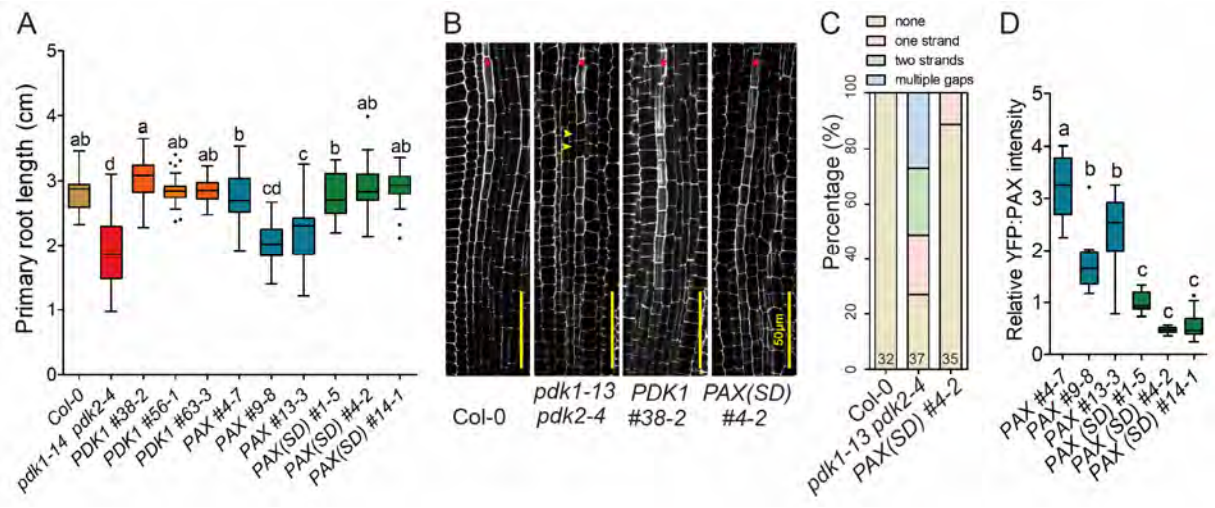

Figure 2. PDK1-dependent activation of PAX directs protophloem differentiation. A-C, *pdk1 pdk2* primary root length of 8-day-old- (A) and PPSE defects of 5-day-old (B, C) wild-type, *pdk1 pdk2*, *pdk1 pdk2 pPDK1::YFP:PDK1 (PDK1), pdk1 pdk2 pPDK1::YFP:PAX (PAX)* or *pdk1 pdk2 pPDK1::YFP:PAX(SD) (PAX(SD))* seedlings. 22 to 36 seedlings were measured for each line in (A). The red asterisks mark the protophloem cell layer, yellow arrowheads point out gap locations in (B). Numbers in columns of (C) represent the number of observed roots. D, Relative *PAX* expression level in the indicated lines, as determined by the YFP:PAX fluorescence intensity in columella cells. The average intensity in line *YFP:PAX(SD)#1-5* was put at 1. Statistically different groups in (A, D) are indicated with lower case letters, as determined by a One-way ANOVA followed by Tukey's test ($p < 0.05$). The whiskers are plotted with Tukey's method.

pdk1 pdk2 cotyledon defects uncover a more general role for PDK1 in vascular development

The fragmented pattern of *pDR5::GUS* expression in *pdk1 pdk2* mutant cotyledons (Chapter 2) suggested that *PDK1* and *PDK2* are also involved in vascular development in cotyledons. Compared to other known mutants with cotyledon vein defects, *pdk1 pdk2* cotyledons exhibited a unique, highly fragmented vein pattern similar to that in *scarface* (*scf-9*) or *gnom*/*emb30-1* mutants (Figure 3) (Richter et al., 2010). Fused *pdk1 pdk2* cotyledons showed even stronger defects with both fusion and fragmentation (Figure 3C). Even though D6PK/D6PKLs are PDK1 *in vitro* phosphorylation targets and fused cotyledons are also observed for *d6pk012* triple mutant seedlings, dissimilar vein patterns between these two mutants suggested that PDK1 controlled vascular development in cotyledons may not be predominantly dependent on D6PK/D6PKLs (Figure 3C, I) (Zegzouti et al., 2006). Meanwhile, vein patterning was largely restored in *PAX(SD) pdk1 pdk2* cotyledons, although some cotyledons showed few fragments and discontinued loops (Figure 3M). We also observed that

PAX(SD) pdk1 pdk2 plants developed relatively expanded rosette leaves when grown in the soil, compared to *pdk1 pdk2* plants, while *PAX pdk1 pdk2* did not (Figure S2). These results imply that PDK1-mediated PAX phosphorylation signaling is not limited to root (pro)vascular tissues, but occurs more globally during vascular development.

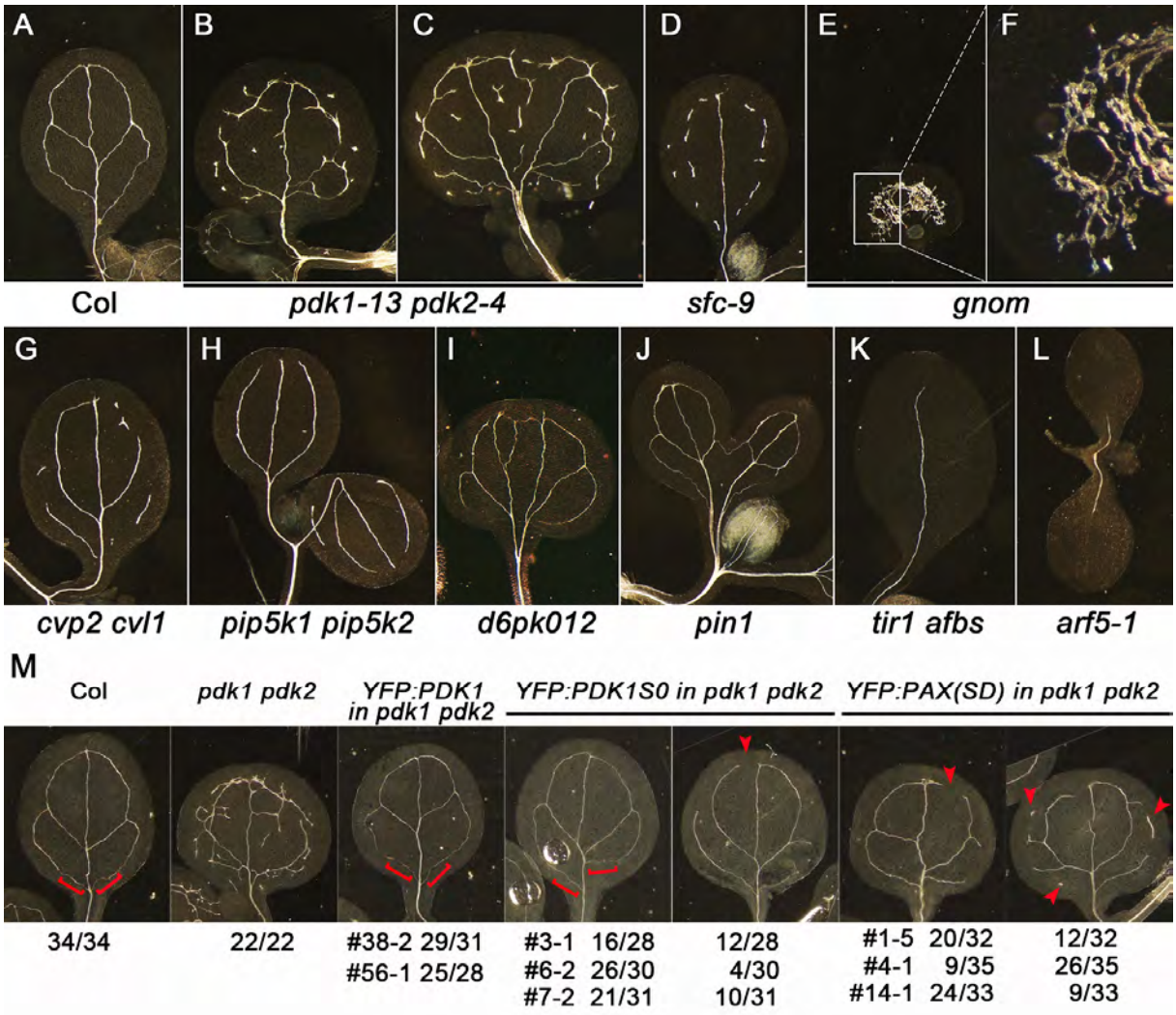

Figure 3. The unique *pdk1-13 pdk2-4* mutant cotyledon vein pattern can be partially rescued by *PDK1S0* and *PAX(SD)*. A-L, Dark-field images showing the vein pattern of cleared cotyledons of 7-day-old seedlings of wild-type Arabidopsis (Col-0) or the indicated mutants (below image). For each line a representative image was selected from >50 observed cotyledons. *tir1 afbs*: *tir1-1 afb1-3 afb2-3 afb3-4* (K). M, *pPDK1::YFP:PDK1S0* and *pPDK1::YFP:PAX(SD)* partially rescued cotyledon vein breaks in *pdk1 pdk2*. The fraction of the total number of observed cotyledons showing a similar phenotype is indicated below each image. Cotyledons showing vein pattern breaks at positions indicated with red brackets are classified into the same group as cotyledons with continuous veins. The red arrow heads point out break locations and isolated islands.

PDK1 PH domain and polar membrane localization are not essential for its role in vascular development

PDK1 co-localizes with PAX at the basal side of the root protophloem cells, thereby providing the opportunity for the two proteins to interact (Figure 4D). However, PAX basal localization does not seem to be dependent on its interaction with PDK1, nor on its phosphorylation status, as PAX and PAX(SD) show the same polar localization at the PM (Figure 4D). To study the contribution of PDK1 basalization on this signaling pathway, we expressed a YFP tagged

PDK1 splice variant product PDK1S0 lacking the PH domain, under the *PDK1* promoter in the *pdk1 pdk2* background. The fragmented vein pattern in the cotyledon of *pdk1 pdk2* was rescued to wild-type-like or random-break loops by *PDK1S0* (Figure 3M). Moreover, a complete rescue of primary root elongation and PPSE differentiation and a partial restoration of the lateral root emergence was also observed in *YFP:PDK1S0 pdk1 pdk2* seedlings (Figure 4A, B, C; Figure S1). This indicates that PH domain-directed basal PDK1 localization is not essential for vascular development and primary root growth. Most likely, PAX provides a co-localization and interaction site for PDK1S0 at the basal side of root protophloem cells, and possibly the higher kinase activity of the PDK1S0 version (Figure 5B) can compensate for the lack of immediate co-localization with the PAX substrate. The PH domain has been proposed to be characteristic for PDK1 in vascular plant species (Dittrich and Devarenne, 2012). Based on our results, however, we reexamined the PDK1 protein sequences in several non-vascular and vascular plants. Although all flowering plant PDK1 proteins contain a C-terminal PH domain, the PDK1 proteins in some ferns (*Sceptridium dissectum* and *Plagiogyria japonica*) do not, while these ferns do develop vascular tissue. The PDK1 ortholog of the green algae *Prasinococcus capsulatus* does have a PH domain (Figure 4E), suggesting that the ancestral plant PDK1 did have a PH domain, and that this domain has been lost in some early non-seed plant classes, but is maintained in flowering plants. In conclusion, this evolutionary analysis shows that the PH domain in PDK1 is not specific for vascular plants.

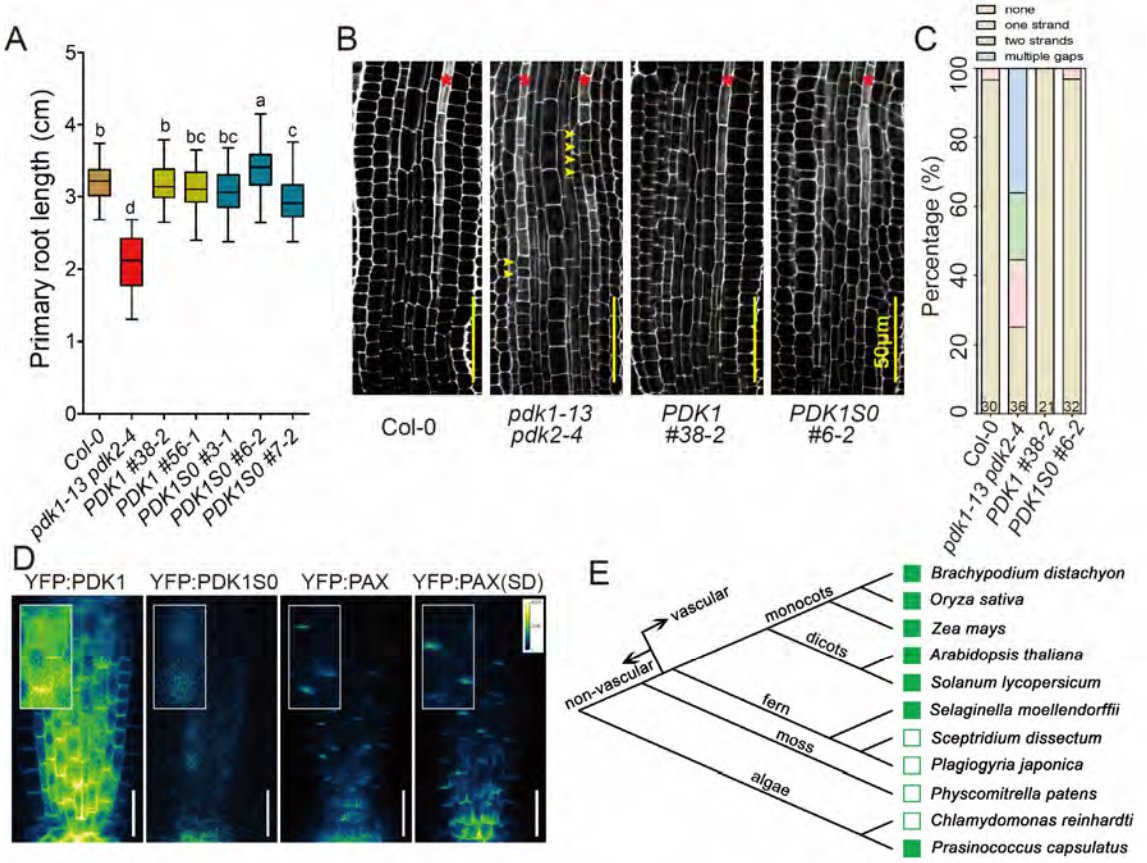

Figure 4. The PH domain is not essential for PDK1 function in the auxin sensing rheostat during vascular development. A-C, *pdk1 pdk2* primary root length (A) and PPSE (B, C) defects are complemented by PDK1S0. 34 to 42 8-day-old seedlings were measured for each line (A). The red asterisks mark the protophloem cell layer, yellow arrowheads point out gap locations in (B). Numbers in columns of (C) represent total counts of observed roots. D, Subcellular localization of YFP:PDK1, YFP:PDK1S0, YFP:PAX and YFP:PAX(SD) in *pdk1 pdk2* mutant stele cells. Bar = 20 µm. E, Phylogenetic analysis of the PDK1 protein sequences from different plant species. The solid or hollow green box means PDK1 encompasses or lacks a PH domain, respectively.

PDK1 is strictly regulated at the post-transcriptional level

Our results show that PDK1 is part of an auxin-sensing rheostat that modulates polar auxin transport during vascular development. This raised the question whether PDK1 is regulated by auxin. Quantitative RT-PCR result did not show any effect on *PDK1* transcription up to 4 hours after auxin treatment (Figure 5A). Also, no significant change in the production of the splice variant coding for the shorter but more active PDK1S0 protein version (lacking the PH domain) was detected after auxin treatment (Figure 5B, C). The phospholipids PI(4,5)P2 and phosphatidic acid (PA) have been reported to bind PDK1 and allow its association with the PM (Deak et al., 1999; Anthony et al., 2004). Applying phosphoinositide biosynthesis inhibitors wortmannin (WM), phenylarsine oxide (PAO), but not the PA biosynthesis inhibitor 1-butanol, strikingly disrupted YFP:PDK1 basal PM localization, suggesting that phosphoinositide may play a more dominant role than PA in YFP:PDK1 PM targeting (Figure 5D, G-I). Treatment with the fungal toxin Brefeldin A (BFA), a specific inhibitor of the ARF-GEF GNOM, also recruited YFP:PDK1 from the PM to the cytosol, suggesting that GNOM-mediated recycling is crucial for the basal localization of YFP:PDK1 in root stele cells (Figure 5D, F). Phospholipid biosynthesis and GNOM-mediated membrane trafficking have been reported to be enhanced by auxin (Geldner et al., 2003; Tejos et al., 2014). However, when treated with IAA, YFP:PDK1 protein abundance on the PM was not noticeably changed (Figure 5D, E).

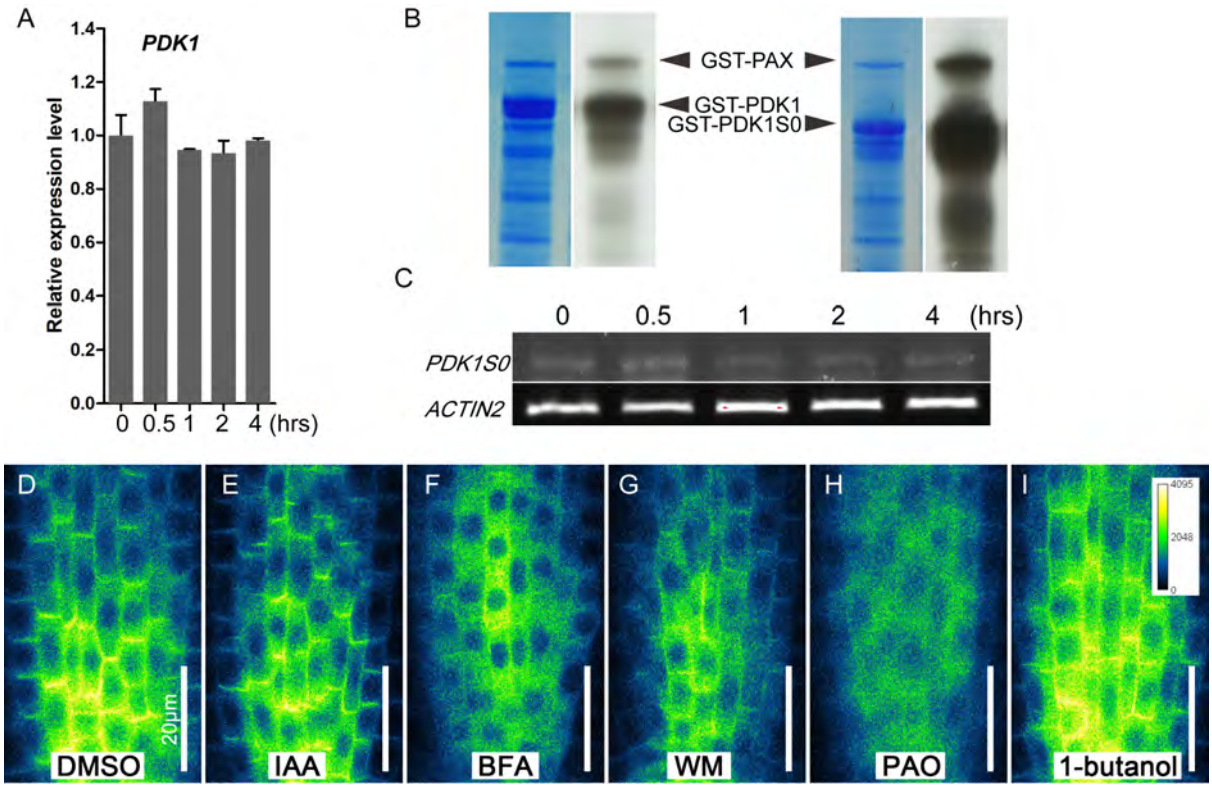

Figure 5. PDK1 is regulated at the post-transcriptional level. A, Relative *PDK1* transcript levels (including the different splicer variants) is not significantly changed in 5-day-old seedlings following 0.5 to 4 hours treatment with 1 µM IAA. B, *In vitro* phosphorylation assay showing GST-PDK1/PDK1S0 autophosphorylation and GST-PAX transphosphorylation. PageBlue stained gel (left) and autoradiograph (right) are shown, and positions of the GST-tagged PAX, -PDK1 and -PDK1S0 are indicated. C, Abundance of the *PDK1S0* splice variant is not strikingly altered in 5 day-old-seedlings after 0.5 to 4 hours treatment with 1µM IAA. D-I, Confocal images of *pdk1 pdk2 pPDK1::YFP-PDK1* roots showing YFP-PDK1 localization after 1 hour treatment with DMSO (D), 1 µM indole-3-acetic acid (IAA)(E), 50 mM brefeldin A (BFA)(F), 33 µM wortmannin (WM)(G) or 0.1% 1-butanol (I), or 30 min treatment with 30 µM phenylarsine oxide (PAO)(H).

Discussion

The development of vascular tissue has been a very helpful innovation for plants in their endeavors to colonize the land. By providing connections between different organs and tissues, vascular tissues allow these organs to communicate with each other and to exchange nutrients and functionally diversify, and in the end, plants to become bigger and more versatile. By using reverse genetics, we verified that two highly conserved protein kinases in eukaryotes Arabidopsis *PDK1* and *PDK2* are involved in the vascular development in cotyledons and roots. Our data does point to a role for PDK1 in phosphorylating and activating AGC1 kinase PAX, as part of an auxin sensing molecular rheostat that controls polar auxin transport during vascular development, in roots and cotyledons. PAX is central to this rheostat as it enhances auxin efflux by phosphorylating PIN proteins in their large hydrophilic loop (Figure 6A, B). At low auxin levels, PAX activation by PDK1 is prevented by BRX binding, resulting in limited auxin efflux (Figure 6A). As a consequence, auxin levels in the cell rise, leading to dissociation of BRX, thereby allowing PDK1 to promote auxin efflux by activating PAX by phosphorylation (Figure 6B). Auxin treatment did not significantly enhance PDK1 basal PM localization in root stele cells. This indirectly suggests that either auxin-controlled phospholipid biosynthesis might be rate-limiting for PAX polarity or for PDK1 kinase activity (Anthony et al., 2004). The similarities in cotyledon vein fragmentation between *pdk1 pdk2, cvp2 cvl1* and *pip5k1 pip5k2* mutants do suggest that phospholipids are part of the auxin transport controlling regulatory pathway. Most likely they are necessary for the PM association of PAX and of other AGC1 clade kinases downstream of PDK1. Moreover, since the PDK1S0 isoform is clearly more active than full length PDK1 in auto- and transphosphorylation *in vitro*, alternative splicing of *PDK1* transcripts might provide a mechanism for balancing the phospholipid requirement of PDK1 activity under specific growth conditions or in certain developmental processes. Polar localization does not contribute too much to proper PDK1 function in root protophloem differentiation. Similarly, apical localization of OPS is not crucial for its function in vascular differentiation (Breda et al., 2017). Evolutional analysis of PDK1 also excluded the co-relationship between PH-domain and the occurrence of vascular tissue in land plants, which is different from the co-emergence of the *OPS* gene and sieve elements (Breda et al., 2017).
Auxin-transport dependent canalization has since long been accepted as a hypothesis for vascular pattern formation. But direct disturbance of auxin transport (*pin1* or NPA treatment) or -signaling (*tir1 afbs* or *arf5*) leads to very different vein pattern defects compared to what is observed for *pdk1 pdk2*, *cvp2 cvl1*, *pip5k1 pip5k2*, *sfc* or *gnom* mutants, in which auxin transport is affected indirectly (Mattsson et al., 1999; Aida et al., 2002; Sieburth et al., 2006; Carland and Nelson, 2009; Naramoto et al., 2009; Richter et al., 2010; Tejos et al., 2014). Here we explain these two types of disturbances in vein pattern formation with a direction-independent or a direction-dependent reduction of auxin flow. In the direction-dependent reduction of auxin transport in the *cvp2 cvl1* mutant, for example, altered accumulation of polarly localized phosphoinositide affects the proper polar localization of PM-associated regulatory proteins, leading to a decrease in auxin transport only in that polar direction. This causes the “mainstream” of auxin to be randomly divided into local auxin sinks, where rapid differentiation of provascular cells leads to vein fragments that are still arranged in a similar pattern as in wild type. In contrast, in direction-independent interference, e.g, by NPA treatment or loss of PIN function, auxin transport is evenly decreased in all directions, leading to reduced

canalization and thus to a more diffuse auxin stream, causing major changes in the vascular pattern and fused veins. Similarly, in auxin signaling mutants auxin sensitivity is evenly decreased in all cells of a tissue, thus leading to changes in vascular pattern and fused veins rather than to interrupted veins in a similar pattern as wild type. This hypothesis seems also true for root protophloem differentiation. Although the polarity of PDK1 itself does not seem to contribute to direction-dependent promotion of auxin transport, the obvious basal localization of its substrate PAX does. Our results suggest that during cotyledon vein patterning, PDK1 also interacts with the polar localized PAX to achieve its biological function. Recent data indicates that auxin-induced vein-formation occurs independent of all known auxin intercellular transporters, including PINs. The results suggest that the ARF-GEF GNOM acts upstream of auxin signaling and auxin transport in vein formation to determine tissue-cell-polarizing, and that, in line with our hypothesis, PIN proteins act as regulators of this differentiation process to detail the vein pattern by canalization (Verna et al., 2019).

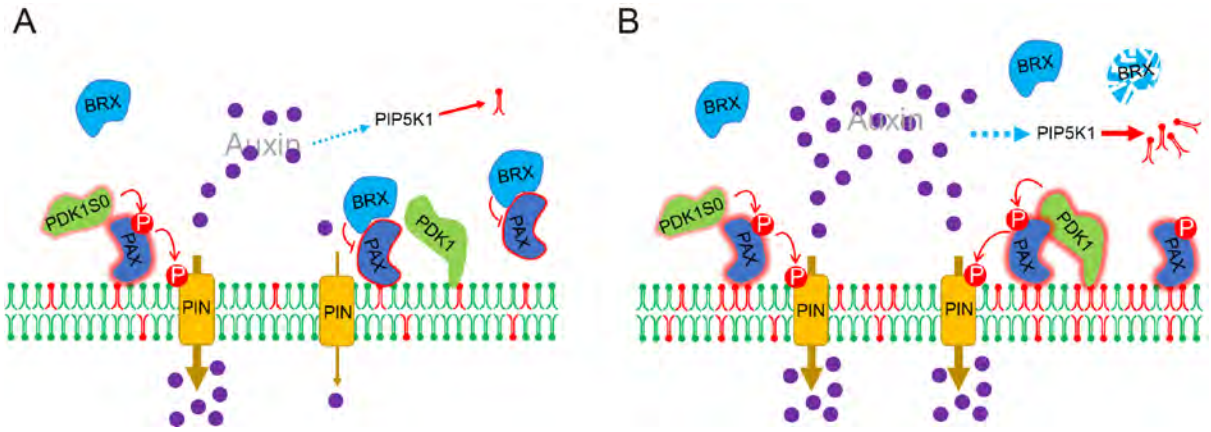

Figure 6. Model showing the role of PDK1 in the auxin sensing rheostat controlling auxin efflux during root protophloem differentiation. Both membrane-localized PDK1 and the cytosolic splice variant PDK1S0 can phosphorylate and activate PAX. When the cellular auxin level is low, PAX is bound by BRX and this prevents its activation by PDK1. Only unbound PAX can be activated by PDK1S0 or PDK1, resulting in limited auxin efflux (A). As cellular auxin levels rise, BRX degradation and subcellular trafficking to the nucleus releases PAX, thereby allowing activation of PAX by PDK1 and the subsequent promotion of auxin efflux by PAX-mediated PIN phosphorylation. In addition, auxin activates PIP5K1 expression and stimulates the PI(4,5)P2 (phospholipid in red) concentration in the PM, resulting in enhanced PDK1 kinase activity (B).

Materials and methods

Plant lines and growth condition

Arabidopsis thaliana (L.) ecotype Columbia 0 (Col-0) was used as wild-type control. *sfc-9* (SALK_069166) (Sieburth et al., 2006), *gnom/emb30-1* (CS6320), *pip5k1 pip5k2* (Tejos et al., 2014), *cvp2 cvl1* (Carland and Nelson, 2009), *d6pk012* (Zourelidou et al., 2009), *pin1* (SALK_047613), *tir1-1 afb1-3 afb2-3 afb3-4* (Parry et al., 2009), *afb5-1* (SALK_023812) have been reported before. *pdk1 pdk2, pPDK1::YFP:PDK1 pdk1 pdk2, pPDK1::YFP:PDK1S0 pdk1 pdk2, pPDK1:turboGFP:GUS* and *pPDK2:turboGFP:GUS are* described in Chapter 2. *pPDK1::YFP:PAX* (*PAX*) and *pPDK1::YFP:PAX(S596D)* (*PAX(SD)*) were transformed into the *pdk1-14(-/-) pdk2-4(+/-)* mutant background. *PAX(SD) pdk1-14(-/-) pdk2-4(-/-)* and homozygous segregated from *PAX pdk1-14(-/-) pdk2-4(+/-)* were used for analysis. Plants in

soil were grown at 16h photoperiod and 70% relative humidity at 21°C. For seedling growth, seeds were vernalized in the dark at 4 °C for 2 days after surface-sterilization, subsequently sown on vertical plates with 0.5×Murashige and Skoog (1/2 MS) medium (Duchefa) containing 0.05% MES, 0.8% agar and 1% sucrose. Plates were placed at 22 °C under 16h photoperiod.

Nucleic acid experiments

RNA was isolated from untreated or auxin treated 5-day-old Col-0 seedlings and using NucleoSpin RNA Plant kit (Macherey Nagel, #740949). Subsequent reverse transcription was performed using the RevertAid RT Reverse Transcription Kit (Thermo Scientific™, #K1691). Auxin treatment was performed in 1/2MS liquid media supplemented with 0.01%DMSO (Mock) or with 1µM IAA dissolved in DMSO. The CFX96 Touch™ Real-Time PCR Detection System (Bio-Rad) and TB Green Premix Ex Taq II (Tli RNase H Plus) (Takara, #RR820B) were used for qRT-PCR experiment. *PDK1* expression was normalized to the reference gene *PP2A-3* (*AT2G42500*) using the ΔΔCt method. For *PDK1S0* RT-PCR, a 38-cycle PCR was followed by *BstZ17*I and *Nsi*I digestion (Thermo Scientific™).
For *PAX* mutagenesis*, PAX* was amplified from Col-0 cDNA and cloned into p*DONR207*, the entry vector was mutated with QuickChange II XL Site-Directed Mutagenesis Kit (Agilent, #200521). *PAX and PAX(S596D)* were then introduced into p*ART27-pPDK1::YFP:gateway* by LR reaction (Invitrogen, Gateway BP/LR Clonase II Enzyme Mix #11789020 and #12538120). p*DNOR207-PAX* was also exchanged into p*GEX-gateway* for *in vitro* protein expression. Primers for nucleic acid experiments are listed in Table S1.

Phenotyping and confocal microscopy

For macroscopic phenotyping, plants in the soil and seedlings were photographed with Nikon D5300. Root length was measured based on these images with ImageJ (Fiji) software. Data was analyzed and plotted into graphs with GraphPad Prism 5.
For observation of the cotyledon vein pattern, 5-day-old seedlings were destained overnight in 70% ethanol and placed on slides with chloral hydrate solution (chloral hydrate: glycerol: water = 4:2:1) for 2-day-clearing. A Leica MZ16FA microscope equipped with dark-field optics and a Leica DFC420C camera was used for photographing.
The modified Pseudo-Schiff Propidium Iodide (mPS-PI) method was employed to stain the cell wall of 5-day-old seedling roots for protophloem observation and quantification (Truernit et al., 2008). Samples were observed using a Zeiss LSM5 Exciter/AxioImager equipped with a 488 nm laser, and the emission signal was collected via a 600nm long pass filter. To quantify gap types, one gap from both strands or more than one gap from both strands were classified into “two strands” or “multiple gaps” group, respectively.
YFP-tagged proteins in the root stele of 4-day-old seedlings were observed using a Zeiss LSM5 Exciter/AxioImager with a 40× oil immersion objective (NA = 1.2). Samples were excited with a 514 nm laser, and the emission signal was captured using a 530-560nm band pass filter. For YFP-PDK1 subcellular localization analysis, 4-day-old seedlings were treated with 0.1%DMSO (mock), 50 µM brefeldin A (BFA, #B7651, Sigma-Aldrich), 33 µM wortmannin (WM, #W1628, Sigma-Aldrich) 1 µM indole-3-acetic acid (IAA, #I0901, Duchefa Biochemie) or 0.1%

1-butanol (#281549, Sigma-Aldrich) for 1 hour or 30 μM phenylarsine oxide (PAO, #P3075, Sigma-Aldrich) for 30 min in1/2MS liquid medium before microscopy observation.

Phylogenetic analysis

Protein sequences of *PDK1* homologous genes from following species were obtained from the National Center for Biotechnology Information (NCBI): *Solanum lycopersicum* (Gene ID: 544184), *Zea mays* (Gene ID: 100384040), *Oryza sativa* (Gene ID: 4324953), *Brachypodium distachyon* (Gene ID: 100835821), *Physcomitrella patens* (Gene ID: 112277681), *Selaginella moellendorffii* (Gene ID: 9631841), *Chlamydomonas reinhardti* (Gene ID: 5726920), *Arabidopsis thaliana* (Gene ID: 830330). The remaining three PDKs from *Plagiogyria japonica* (onekp:UWOD_scaffold_2139095), *Sceptridium dissectum* (onekp:EEAQ_scaff-old_2087606) and *Prasinococcus capsulatus* (onekp:XMCL_scaffold_2001871) were obtained from data for the 1,000 Plants (1KP) project (http://www.onekp.com). 11 sequences were aligned by ClustalW in MEGA-X, and the phylogenetic tree was constructed by maximum-likelihood procedure. At the same time, the secondary protein structures were predicted by InterPro online tool (https://www.ebi.ac.uk/interpro/).

Other experiments

Histochemical staining of Promoter-GUS reporter lines for GUS activity and *in vitro* phosphorylation assays were performed as described in Chapter 2 or as published (Huang et al., 2010). A Leica MZ16FA microscope with DIC optics was used to observe the GUS staining photographing.

Acknowledgments

We thank Antia Rodriguez-Villalon, Christian Hardtke, Claus Schwechheimer, Ingo Heilmann and Jingke Chang (Jia Li's lab) for providing *cvp2 cvl1, pax paxl*, *d6pk012, pip5k1 pip5k2 and gnom* mutants respectively. We thank Gerda Lamers and Joost Willemse for helping with microscopy work. We are grateful to Nick Surtel, Ward de Winter and Jan Vink for daily technical support. This project was supported by the China Scholarship Council.

Supplementary data

Figure S1. Complementation of the *pdk1 pdk2* mutant by *pDPK1* promoter driven *YFP:PDK1*, *YFP:PDK1S0* or *YPF:PAX(SD)* expression. A-O, Phenotype of 13-day-old seedlings of the indicated lines grown on vertical plates. *pdk1 pdk2 pPDK1::YFP-* is omitted in (D-O) for presentation purpose. Note that YFP-PAX only shows partial complementation in the high expressing line #4.7 (see also Figure 2A).

Figure S2. *pPDK1::YFP:PAX (SD)* partially rescues the decreased rosette diameter of *pdk1-14 pdk2-4*, but *pPDK1::YFP:PAX* does not. Rosette phenotype of 26-day-old wild-type (Col-0), *pdk1-14 pdk2-4* mutant, and *pPDK1::YFP:PAX pdk1-14 pdk2-4* (A) and *pPDK1::YFP:PAX pdk1-14 pdk2-4* (B) plants from several independent transgenic lines.

Table S1. Primers used in this research

usage	primer name	sequence
cloning	PAX-attB1	GGGGACAAGTTTGTACAAAAAAGCAGGCTTCATGCTGGAAATGGAAAGAGTTG
cloning	PAX-attB2	GGGGACCACTTTGTACAAGAAAGCTGGGTTTTAGAAAAACTCAAAGTCTAGAA
mutagenesis	PAX-S596D-FP	AACACACGGTCCATGGACTTTGTTGGAACCCAC
mutagenesis	PAX-S596D-RP	GTGGGTTCCAACAAAGTCCATGGACCGTGTGTT
qRT	qRT-PDK1-FP	CGGTGCTAATGTTTCTAGAAGC
qRT	qRT-PDK1-RP	CTTCTTCTTTGCCCTAACAACC
qRT	PP2A-3-qRT-FP	GATGGATACAACTGGGCTCACG
qRT	PP3A-3-qRT-RP	TCGGTGCTGGTTCAAACTGG
RT	PDK1FL-FP-BamHI	CGGGATCCCGATGTTGGCAATGGAGAAAGAATTTG
RT	PDK1S0-RP-EcoRI	CGGAATTCCGTTAGGAGCTTTGAACAAGGTTGCT
RT	ACTIN2-RT-FP	TGAGACCTTTAACTCTCCCGCTA
RT	ACTIN2-RT-RP	TGATTTCTTTGCTCATACGGTCA

References

Aida, M., Vernoux, T., Furutani, M., Traas, J., and Tasaka, M. (2002). Roles of PIN-FORMED1 and MONOPTEROS in pattern formation of the apical region of the Arabidopsis embryo. Development **129**: 3965–74.

Anne, P., Azzopardi, M., Gissot, L., Beaubiat, S., Hématy, K., and Palauqui, J.C. (2015). OCTOPUS negatively regulates BIN2 to control phloem differentiation in Arabidopsis Thaliana. Curr. Biol. **25**: 2584–2590.

Anne, P. and Hardtke, C.S. (2018). Phloem function and development — biophysics meets genetics. Curr. Opin. Plant Biol. **43**: 22–28.

Anthony, R.G., Henriques, R., Helfer, A., Mészáros, T., Rios, G., Testerink, C., Munnik, T., Deák, M., Koncz, C., and Bögre, L. (2004). A protein kinase target of a PDK1 signalling pathway is involved in root hair growth in Arabidopsis. EMBO J. **23**: 572–581.

Barbosa, I.C.R., Zourelidou, M., Willige, B.C., Weller, B., and Schwechheimer, C. (2014). D6 PROTEIN KINASE activates auxin transport-dependent growth and PIN-FORMED phosphorylation at the plasma membrane. Dev. Cell **29**: 674–685.

Bauby, H., Divol, F., Truernit, E., Grandjean, O., and Palauqui, J.C. (2007). Protophloem differentiation in early Arabidopsis thaliana development. Plant Cell Physiol. **48**: 97–109.

Breda, A.S., Hazak, O., and Hardtke, C.S. (2017). Phosphosite charge rather than shootward localization determines OCTOPUS activity in root protophloem. Proc. Natl. Acad. Sci. **114**: E5721–E5730.

Carland, F. and Nelson, T. (2009). CVP2- and CVL1-mediated phosphoinositide signaling as a regulator of the ARF GAP SFC/VAN3 in establishment of foliar vein patterns. Plant J. **59**: 895–907.

Deak, M., Casamayor, A., Currie, R.A., Peter Downes, C., and Alessi, D.R. (1999). Characterisation of a plant 3-phosphoinositide-dependent protein kinase-1 homologue which contains a pleckstrin homology domain. FEBS Lett. **451**: 220–226.

Dhonukshe, P., Huang, F., Galvan-Ampudia, C.S., Mähönen, A.P., Kleine-Vehn, J., Xu, J., Quint, A., Prasad, K., Friml, J., Scheres, B., and Offringa, R. (2010). Plasma membrane-bound AGC3 kinases phosphorylate PIN auxin carriers at TPRXS(N/S) motifs to direct apical PIN recycling. Development **137**: 3245–55.

Dittrich, A.C.N. and Devarenne, T.P. (2012). Perspectives in PDK1 evolution: Insights from photosynthetic and non-photosynthetic organisms. Plant Signal. Behav. **7**: 642–649.

Durner, M., Greenberg, D., and Delgado-Escueta, A. (2003). APL regulates vascular tissue identity in Arabidopsis. Nature **42**: 63–67.

Feraru, E. and Friml, J. (2008). PIN polar targeting. Plant Physiol. **147**: 1553–1559.

Friml, J. et al. (2004). A PINOID-dependent binary switch in apical-basal PIN polar targeting directs auxin efflux. Science (80-.). **306**: 862–865.

Furuta, K.M. et al. (2014). Arabidopsis NAC45/86 direct sieve element morphogenesis culminating in enucleation. Science (80-.). **345**: 933–937.

Geldner, N., Anders, N., Wolters, H., Keicher, J., Kornberger, W., Muller, P., Delbarre, A., Ueda, T., Nakano, A., and Jürgens, G. (2003). The Arabidopsis GNOM ARF-GEF mediates endosomal recycling, auxin transport, and auxin-dependent plant growth. Cell **112**: 219–30.

Gray, J.W., Nelson Dittrich, A.C., Chen, S., Avila, J., Giavalisco, P., and Devarenne, T.P. (2013). Two Pdk1 phosphorylation sites on the plant cell death suppressor Adi3 contribute to substrate phosphorylation. Biochim. Biophys. Acta **1834**: 1099–106.

Hazak, O., Brandt, B., Cattaneo, P., Santiago, J., Rodriguez-Villalon, A., Hothorn, M., and Hardtke, C.S. (2017). Perception of root-active CLE peptides requires CORYNE function in the phloem vasculature. EMBO Rep. **18**: 1367–1381.

Huang, F., Kemel Zago, M., Abas, L., van Marion, A., Galván-Ampudia, C.S., and Offringa, R. (2010). Phosphorylation of conserved PIN motifs directs Arabidopsis PIN1 polarity and auxin transport. Plant Cell **22**: 1129–1142.

Kang, Y.H., Breda, A., and Hardtke, C.S. (2017). Brassinosteroid signaling directs formative cell divisions and protophloem differentiation in *Arabidopsis* root meristems. Development **144**: 272–280.

Kang, Y.H. and Hardtke, C.S. (2016). Arabidopsis MAKR 5 is a positive effector of BAM 3 -dependent CLE 45 signaling. EMBO Rep. **17**: 1–10.

Marhava, P., Bassukas, A.E.L., Zourelidou, M., Kolb, M., Moret, B., Fastner, A., Schulze, W.X., Cattaneo, P., Hammes, U.Z., Schwechheimer, C., and Hardtke, C.S. (2018). A molecular rheostat adjusts auxin flux to promote root protophloem differentiation. Nature **558**: 297–300.

Mattsson, J., Sung, Z.R., and Berleth, T. (1999). Responses of plant vascular systems to auxin transport inhibition. Development **126**: 2979–91.

Miyashima, S. et al. (2019). Mobile PEAR transcription factors integrate positional cues to prime cambial growth. Nature **565**: 490–494.

Mouchel, C.F., Briggs, G.C., and Hardtke, C.S. (2004). Natural genetic variation in Arabidopsis identifies BREVIS RADIX, a novel regulator of cell proliferation and elongation in the root. Genes Dev. **18**: 700–714.

Naramoto, S., Sawa, S., Koizumi, K., Uemura, T., Ueda, T., Friml, J., Nakano, A., and Fukuda, H. (2009). Phosphoinositide-dependent regulation of VAN3 ARF-GAP localization and activity essential for vascular tissue continuity in plants. Development **136**: 1529–1538.

Parry, G., Calderon-Villalobos, L.I., Prigge, M., Peret, B., Dharmasiri, S., Itoh, H., Lechner, E., Gray, W.M., Bennett, M., and Estelle, M. (2009). Complex regulation of the TIR1/AFB family of auxin receptors. Proc.

Natl. Acad. Sci. **106**: 22540–22545.

Richter, S., Anders, N., Wolters, H., Beckmann, H., Thomann, A., Heinrich, R., Schrader, J., Singh, M.K., Geldner, N., Mayer, U., and Jürgens, G. (2010). Role of the GNOM gene in Arabidopsis apical-basal patterning - From mutant phenotype to cellular mechanism of protein action. Eur. J. Cell Biol. **89**: 138–144.

Rodriguez-Villalon, A., Gujas, B., van Wijk, R., Munnik, T., and Hardtke, C.S. (2015). Primary root protophloem differentiation requires balanced phosphatidylinositol-4,5-biphosphate levels and systemically affects root branching. Development **142**: 1437–1446.

Ruiz Sola, M.A., Coiro, M., Crivelli, S., Zeeman, S.C., Schmidt Kjølner Hansen, S., and Truernit, E. (2017). OCTOPUS-LIKE 2, a novel player in Arabidopsis root and vascular development, reveals a key role for OCTOPUS family genes in root metaphloem sieve tube differentiation. New Phytol. **216**: 1191–1204.

De Rybel, B., Mähönen, A.P., Helariutta, Y., and Weijers, D. (2016). Plant vascular development: From early specification to differentiation. Nat. Rev. Mol. Cell Biol. **17**: 30–40.

Scacchi, E., Salinas, P., Gujas, B., Santuari, L., Krogan, N., Ragni, L., Berleth, T., and Hardtke, C.S. (2010). Spatio-temporal sequence of cross-regulatory events in root meristem growth. Proc. Natl. Acad. Sci. **107**: 22734–22739.

Sieburth, L.E., Muday, G.K., King, E.J., Benton, G., Kim, S., Metcalf, K.E., Meyers, L., Seamen, E., and Van Norman, J.M. (2006). SCARFACE encodes an ARF-GAP that is required for normal auxin efflux and vein patterning in Arabidopsis. Plant Cell **18**: 1396–411.

Tejos, R., Sauer, M., Vanneste, S., Palacios-Gomez, M., Li, H., Heilmann, M., van Wijk, R., Vermeer, J.E.M., Heilmann, I., Munnik, T., and Friml, J. (2014). Bipolar plasma membrane distribution of phosphoinositides and their requirement for auxin-mediated cell polarity and patterning in Arabidopsis. Plant Cell **26**: 2114–2128.

Truernit, E., Bauby, H., Belcram, K., Barthelemy, J., and Palauqui, J.-C. (2012). OCTOPUS, a polarly localised membrane-associated protein, regulates phloem differentiation entry in Arabidopsis thaliana. Development **139**: 1306–1315.

Truernit, E., Bauby, H., Dubreucq, B., Grandjean, O., Runions, J., Barthelemy, J., and Palauqui, J.-C. (2008). High-resolution whole-mount imaging of three-Dimensional tissue organization and gene expression enables the study of phloem development and structure in Arabidopsis. Plant Cell **20**: 1494–1503.

Verna, C., Ravichandran, S.J., Sawchuk, M.G., Linh, N.M., and Scarpella, E. (2019). Coordination of tissue cell polarity by auxin transport and signaling. bioRxiv: 680090.

Wallner, E.S. et al. (2017). Strigolactone- and karrikin-independent SMXL proteins are central regulators of phloem formation. Curr. Biol. **27**: 1241–1247.

Zegzouti, H., Li, W., Lorenz, T.C., Xie, M., Payne, C.T., Smith, K., Glenny, S., Payne, G.S., and Christensen, S.K. (2006). Structural and functional insights into the regulation of Arabidopsis AGC VIIIa kinases. J. Biol. Chem. **281**: 35520–35530.

Zourelidou, M. et al. (2014). Auxin efflux by PIN-FORMED proteins is activated by two different protein kinases, D6 PROTEIN KINASE and PINOID. Elife **3**: 1–25.

Zourelidou, M., Muller, I., Willige, B.C., Nill, C., Jikumaru, Y., Li, H., and Schwechheimer, C. (2009). The polarly localized D6 PROTEIN KINASE is required for efficient auxin transport in Arabidopsis thaliana. Development **136**: 627–636.